UNIVERSITY OF CAPE TOWN

Department of Mechanical Engineering
Rondebosch, Cape Town, South Africa

BLAST IMPACT AND SURVIVABILITY RESEARCH UNIT

BISRU

IMPULSE LOADING OF NEAR-FIELD SHALLOW-BURIED EXPLOSIONS

Frans Jacobus Beetge

MARCH 2008

A dissertation submitted in partial fulfilment of the requirements
for the degree MSc (Engineering)

DECLARATION

I, Frans Jacobus Beetge, declare that this dissertation is essentially my own work, except where reference or acknowledgement is made to contribution by others. It is being submitted in partial fulfilment of the requirements for the Master of Science in Engineering degree at the University of Cape Town, and has not before been submitted in this or any other form for a degree at any University.

Frans Jacobus Beetge

March 2008

The whole is often more than the
sum of its parts.
— Aristotle

ABSTRACT

Prediction of the total impulse for a mine-protected vehicle must be empirically determined for South African Paardefontein soil pit soil at the start-up phase of a new vehicle project, particularly when experimental data are not yet available for the calibration of computational efforts.

The total impulse on a mine-protected vehicle is influenced by a number of factors, such as size of the exposed target area, explosive mass, explosive diameter to height ratio, standoff distance, depth of burial, and soil properties.

This investigation entails the development of an empirical equation for predicting total impulse by applying regression analysis. A series of comparative test results were obtained with the Scientific Instrumented Impulse Measurement Apparatus (SIIMA) for TNT equivalent surrogate mines of 2.13 kg – 8 kg mass and diameter to height ratio of 5:1, and are reported.

The lethal aspects of buried mines (target loading mechanisms), such as the detonation shock load, impact load and distributed load, are identified and discussed. Important parameters influencing anti-vehicular blasts, such as standoff distance, soil effects, mine composition and geometry and target shape, are investigated and reported.

In conclusion, a SIIMA empirical equation is established which, although limited in standoff distance, can be used as an affordable and quick tool to calculate the vertical impulse on a flat bottom mine-protected vehicle. The SIIMA results show reasonable agreement with the published data of Westine et al (1985) (Braid [1], Williams et al [2] and Williams and Poon [3]), and with the computational predictions provided by the CSIR DPSS-LS.

The results provide a better understanding of the complex behaviour of shallow-buried mines in dry sand as an anti-vehicular mine threat, when considering parameters such as standoff distance and depth of burial for constant conditions of explosive aspect ratio (diameter to height values).

TABLE OF CONTENTS

LIST OF FIGURES

LIST OF TABLES

NOTATION

Lower Case

a_1 = Speed of sound

a = Standoff distance, parameter or variable

b = Width of the moving-mass or decay constant

c = Height of the explosive, or coefficient of damping or seismic P-wave velocity in the soil, or speed of sound of a shock wave

d = Bump-stop displacement, or depth of burial of the mine – from ground level to the top of the mine, or depth of burial of the mine – from ground level to the centre of the mine, or lateral distance from the target point to centre of mine

e = Base of natural logarithms

g = Gravity

h = Standoff distance – from ground level to the bottom of the target

i_r = Reflected impulse

i_z, i_V = Specific vertical impulse or impulse per unit area

i_{SO} = Specific impulse, meaning impulse per unit area

k = Spring constant or factor for SIIMA moving-mass or tamping of soil in the Gurney equation

m = Mass

m_c = Mass of explosive charge

r = Distance to location of impulse prediction or distance travelled from explosion

t = Time

t_A = Time of arrival

t_O = Positive phase duration

t_G = End of the positive phase and beginning of the negative phase

t_S = Negative phase duration

t_N = End of the negative phase

t_{SF} = Time required for shock wave development

x = Displacement

v_g = Characteristic Gurney velocity of TNT (2440 m/s)

v = Velocity

w = Nut displacement (distance wound down shaft)

x_i = The independent, or predictor variable

y_i = The dependent, or response variable of the ith data point

z = Standoff distance – from the bottom of the target to the centre of the mine

Upper Case

A = Cross-sectional area of the charge

A_{MINE} = Cross-sectional area of the mine

A_p = Known plug end area

C_p = Specific heat at constant pressure

C_v = Specific heat at constant volume

CL = Confidence limit

D = Velocity of detonation

D_{mine} = Diameter of the mine

E = Total energy of the explosive, or internal energy of the gas

E_O = Initial explosion energy

E_K = Kinetic energy of the ground

E_G = Energy of the detonation products

E_{EL} = Energy of soil elastic deformation

E_D = Soil dissipation energy = $E_M + E_T$

E_M = Mechanical energy losses

E_T = Thermal energy losses

F = Force

H = Specific enthalpy

I_Z = Scaled impulse

I_M = Up-scaled impulse

I, I_z = Total impulse

I_t = Total impulse (N-s)

K = Bulk modulus of the soil

L_W = Positive wavelength

M, M_1, M_2 = Shock Mach number

P(t) = Instantaneous static overpressure at any given time t

P = Pressure

$P_{TOTAL} = P_{SO} + P_{DYN} = P_{STAG}$ = total pressure

P_{SO} = Peak incident overpressure or peak static overpressure or side-on pressure

P_S = Absolute peak pressure, dimensionless location indicator

P_a = Atmospheric pressure (±101.325 kPa)

P_{DYN} = Peak dynamic overpressure

P_{REF} = Peak reflective overpressure

P_{OVER} = Peak overpressure

P_{STAG} = Peak stagnation overpressure

P_R = Reflected pressure

P_m = Known plug mass

P_v = Measured plug velocity

R_C = Reflection coefficient

R = Distance from the centre of the charge or gas constant for unit mass

R_O = The radius of the explosive charge

S = Standoff distance - from the bottom of the target to the soil surface, or from the bottom of the target to the centre of the mine

T = Absolute temperature

U = Gas velocity

U_s = Shock front velocity

W = Charge mass of the blast in kilogram based TNT equivalence

W = Mass of explosive

X1 = Depth of burial

X2 = Standoff distance

Y = Measured impulse per unit mass

Z = Scaled distance from the charge

Greek Characters

δ = Burial depth – from ground level to the centre of the mine

ρ_{SOIL} = Mass density of the soil

ρ = Density, or mass density of the soil, or air density

ρ_1 = Air density

θ = Time constant

α_i = Angle of incidence

γ = Ratio of specific heats

σ_i = the measurement error or standard deviation of the **i**th data point

χ = merit function

ABBREVIATIONS

BISRU = Blast Impact and Survivability Research Unit

CFD = Computerised Fluid Dynamics

CFAS = Concrete Fine Aggregate Sand

cm = Centimeter

DAS/DAQ = Data Acquisition System

CI = Confidence Interval

CIL = Confidence Interval Limit

CSIR = Council for Scientific and Industrial Research

CL-20 = 2,4,6,8,10,12-hexanitrohexaazaisowurzitane

CY = Cylinder cone

D:H or D/H = Diameter to height ratio

DOB = Depth of burial

DOF = Degree of freedom

DPSS = Defence, Peace, Safety and Security

EFP = Explosively formed projectile

FOX-7 = Diaminodinittrooethylene

FCT = Flux Corrected Transported

HNS = Hexanitrostilbene

HOT = Height of target

HMX = High melting explosive or octogen or cyclotetramethylenetetranitramine

in = Inch

IED = Improvised explosive devices

ITC = Inverted truncated cone

J = Joule

JWL = Jones-Wilkins-Lee

LS = Landwards Sciences

LLM-105 = 2,6-diamino-3,5-dinitropyrazine-1-oxide

lb = Pound

m = Metres

N/A = Not applicable

N = Newton

ob = Overburden

PETN = Pentaerythritol tetranitrate; dry

μs = Microseconds

RDX = Royal demolition explosive or cyclotrimethylenetrinitramine

RHA = Rolled homogeneous armour

SFF = Self-forming fragment

SC = Shaped charge

SIIMA = Scientific Instrumented Impulse Measurement Apparatus

s = Seconds

TATB = 1,3,5-triamino-2,4,6-trinitrobenzene

TNT = 2,4,6-trinitrotoluene

TNH = 99.95% TNT + 0.05% HNS

TC = Truncated cone

VIMF = Vertical Impulse Measurement Fixture

Dreams come true. Without that possibility
nature would not incite us to
have them.
- John Updike

ACKNOWLEDGEMENTS

I would like to take this opportunity to express my sincere thanks to the following people for their support. Without their assistance, this dissertation could not have been written.

Prof. G N Nurick, my supervisor, for his professional guidance and inspiration during my endeavour to conclude my Master's degree in Science Engineering at the University of Cape Town. I will always remember the five major points you mentioned that are necessary to structure a dissertation. Prof. Nurick's insight into this line of research, his passion in managing BISRU as a centre of excellence, and the way in which he inspires his students motivated me to accomplish this work.

Dr Denis Bergeron and Dr Clive Fortier of the DRDC Canada, for proofreading the literature part of this dissertation and for valuable comments and advice.

Dr Francois Naude, for his assistance and encouragement to make the contents of this dissertation my own.

Dr Izak Snyman of the CSIR DPSS-LS, for his valuable time to review this dissertation, his relevant comments and his Autodyn™ computational results.

My previous senior manager at Armscor, Mr Koos Joubert, and my current senior manager at Armscor, Mr Karel Nel, for their interest and support.

Mr David Reinecke, Mr Manfred Eden, Mr Piet Ramaloko and Ms Rayeesa Ahmed of the CSIR DPSS-LS for the SIIMA comparative data.

The effort of Mr G R Turner (senior scientist at the CSIR DPSS-LS), for the redesign and upgrade of SIIMA.

Armscor for sponsoring my student and publishing fees.

Ms Cá Momberg, for formatting the entire document.

Ms Therese Eberlanz, for the language editing.

My mother Kotie, wife Loy, daughter Frances and son Paul, for their love, support and many prayers. How can I ever thank you?

Most importantly, my gratitude goes to my Heavenly Father for giving me the strength and mercy to perform this work.

DEI GRATIA DEO VOLENTE

What we see depends on mainly
what we look for.
— Sir John Lubbock, (1834 – 1913)

1 INTRODUCTION

1.1 Background

Understanding the physics of anti-tank mines and their explosions (blast loading phenomena) is critical to the design of mine-protected vehicles, ultimately for crew survivability. To accurately develop protection systems for personnel and vehicles from a mine blast, it is necessary to understand and quantify the method of impulse transfer from a mine blast to a near-field (approximately between 0.3 m – 5.0 m standoff distance) target. Underestimating the blast energy could result in an insufficient protection system. Conversely, if the blast energy is overestimated, the protection system becomes too costly to produce, or too bulky to use (Hlady [4]).

1.2 Objectives

The objectives of this dissertation can be summarised as follows:

- Firstly, to scan and review open literature for information on anti-vehicular mine explosions close to the ground, on the ground and in shallow soil.
- Secondly, to scan and review any literature found for information on useful empirical equations to predict mine blast loads on mine-protected vehicles.
- Thirdly, to use an apparatus to measure total force versus time of shallow-buried mines in soil in order to integrate the test data to obtain the total impulse for different mine deployment configurations.
- Fourthly, to develop an empirical equation from the captured comparative data. RSA-MIL-STD-37 [5] quotes the TM-57 as the Southern Africa blast mine threat and requires that all mine-protected vehicles be tested with an 8 kg TNH surrogate mine (without a casing) with a diameter to height ratio of 5:1. RSA-

MIL-STD-37 [5] also states that the 8 kg blast mine surrogate shall be positioned such that the mine is covered with 50 mm loose soil on top of the mine. The soil shall be loosely packed and not tamped. Because of the requirement of RSA-MIL-STD-37 [5], the 8 kg surrogate mine will be the main focus of this dissertation. Firstly, it will be compared to the TM-57 anti-vehicular mine in terms of impulse at various depths of burial and standoff distances, and secondly, used to develop an empirical equation using an established measurement method. Until now, the output of both mines has not been compared and the general perception is that the blast load of both should be equal.

- Fifthly and finally, to draw conclusions and make recommendations based on the findings.

1.3 Approach

There are a number of methods to conduct scientific measurements of the applied impulsive loads of an explosion, such as the Canadian Pendulum (Bergeron and Tremblay [6]) or the U.S. Army Vertical Impulse Measurement Fixture called VIMF (Conniff et al [7]). The South African Scientifically Instrumented Impulse Measuring Apparatus, called SIIMA, has been developed by the CSIR DPSS-LS for this purpose and is used to obtain the envisaged comparative data.

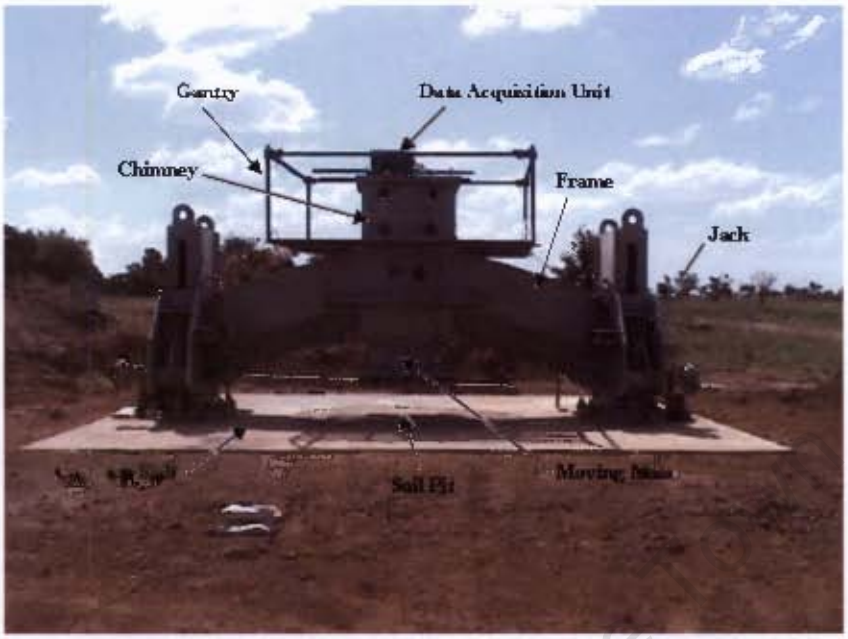

Figure 1.1 Scientifically Instrumented Impulse Measuring Apparatus (SIIMA) (Turner [8])

SIIMA is installed at the Paardefontein test facility (35 km north of Pretoria) and records the total force over time for a maximum explosive charge of up to 8 kg TNT at a standoff distance of 900 mm by means of a damped harmonic oscillator. This force, integrated over time, yields the total impulse for different set-ups, such as varying mine depths of burial, charge sizes, standoff distances and soil densities.

1.4 Process

The process followed in order to complete this dissertation is as follows:

- Scan the Internet and other sources such as libraries and government agencies for information on explosion studies and countermeasures, especially on blast loads directed at near-field targets such as mine-protected vehicles, then review all the literature and condense the findings in the relevant chapters of this dissertation;
- List and analyse all empirical equations and related material obtained;
- Provide a background summary of the Scientific Instrumented Impulse Apparatus (SIIMA);

- Develop a 1-D lumped mass model of SIIMA for analysis;
- Develop an experimental method together with the CSIR DPSS-LS test team to conduct SIIMA comparative tests at Paardefontein;
- Develop a spreadsheet together with the CSIR test team to record the captured SIIMA comparative data;
- Conduct experimental work on SIIMA at the Paardefontein test range together with the CSIR DPSS-LS test team and record the imparted impulse after every test to a planned test matrix to explore the effect of depth of burial, standoff distances and explosive mass;
- Obtain Autodyn™ computational results from Dr I M Snyman (CSIR DPSS-LS).
- Analyse the captured SIIMA comparative data;
- Configure the SIIMA data sets of depth of burial, standoff distances and impulse values in a spreadsheet and plot a 3-D surface graph from which an empirical equation will be obtained that will accurately describe the data (nonlinear curve fitting process);
- Examine and synthesize all relevant data to useable information, and draw the necessary concluding remarks, and
- List the appropriate recommendations to conclude the dissertation.

Once peace is declared the landmine
does not recognise that peace.
— Jody Williams
Nobel Peace Prize Laureate In 1997

2 MOTIVATION FOR STUDY

2.1 Introduction

IEDs and shallow-buried anti-tank mines have become the preferred form of anti-vehicular mine threats in peacekeeping areas. Protection of army vehicles and their occupants against these threats is currently an ***important*** and ***strategic issue*** in the area of defence research. To conduct peacekeeping operations in Southern Africa, the South African Defence Force requires dedicated transport such as mine-protected vehicles to protect their soldiers.

There are still vast numbers of anti-personnel and anti-tank mines deployed in Southern Africa that could remain active for another 30 years. According to statistics of the United Nations (UN) and other non-governmental organizations, more than 60 million landmines are scattered in over 70 countries ([9]). **Figure 2.1** depicts a light unprotected vehicle destroyed by a double anti-vehicular mine. The mine detonated underneath the right front wheel. All five occupants were killed instantly. Mine injuries of vehicle occupants have two main impacts. Firstly, they affect the lives of the casualties and their family (both physically and mentally) and secondly, they have impacts on the medical infrastructure of the affected country.

The main goal of all vehicle designers is to develop mine-protected vehicles that will ensure minimal or, if at all possible, no injuries to the occupants during an anti-vehicular mine incident. Bianchi [10] quotes the following regarding occupant survivability in military vehicles: "***By their very nature, Armoured Fighting Vehicles and Armoured Personnel Carriers are expected to provide their occupants with a level of protection and overall survivability that would more or less***

correspond to the threats the vehicles are expected to encounter during their missions."

Figure 2.1 Damage caused to a light unprotected vehicle by a double mine detonating under the right front wheel (Van Dyk et al [11])

In recent years some initiatives have been undertaken to study and understand mine blast loading in order to enhance the design of vehicles used in mine-affected zones (Fišerová et al [12]). To gain a better understanding this chapter is started by covering fundamentals by reviewing the definition of an explosive material, reviewing the development of military high-explosives since 1800, and lastly, reviewing the TM-57 blast mine which is currently considered to be the main mine threat in Southern Africa.

For an anti-vehicular mine deployed in soil the "vertical" blast load experienced by a mine-protected vehicle, following the detonation of a mine, is due to the transmission of the energy of the blast to its belly through pressure (blast) wave propagation through the soil and air and through momentum transfer from the blast (soil, detonation products and shrapnel) ejecta. According to Braid [1], a study was conducted by Westine et al (1985) wherein it was assumed that the detonation of a mine in soil would produce an impulsive loading on whatever was above it. This loading, it was hypothesized, would be the result of the impact of the expanding soil and explosive

products generated by the detonation. In general, the process was seen as a high-pressure, short-duration event.

2.2 What is an explosive material?

To contemplate the behaviour of anti-vehicular mines, the general behaviour of an explosive material has to be defined, for example, "An explosive is a material, either a pure single substance or a mixture of substances, which is capable of producing an explosion by its own energy" (Davis [13]).

2.3 The evolution of military "high" explosives

It is evident from all literature that trinitrotoluene (TNT) has been the most common conventional military explosive during the 20th century and has traditionally been used to fill anti-vehicular mines. **Figure 2.2** illustrates the various important military high-explosives developed since 1800 as well as an estimation of the relative explosive energy in TNT units, i.e. 200 explosive energy units is 2 times the explosive energy of TNT (or put differently, 2 times 100 explosive energy units).

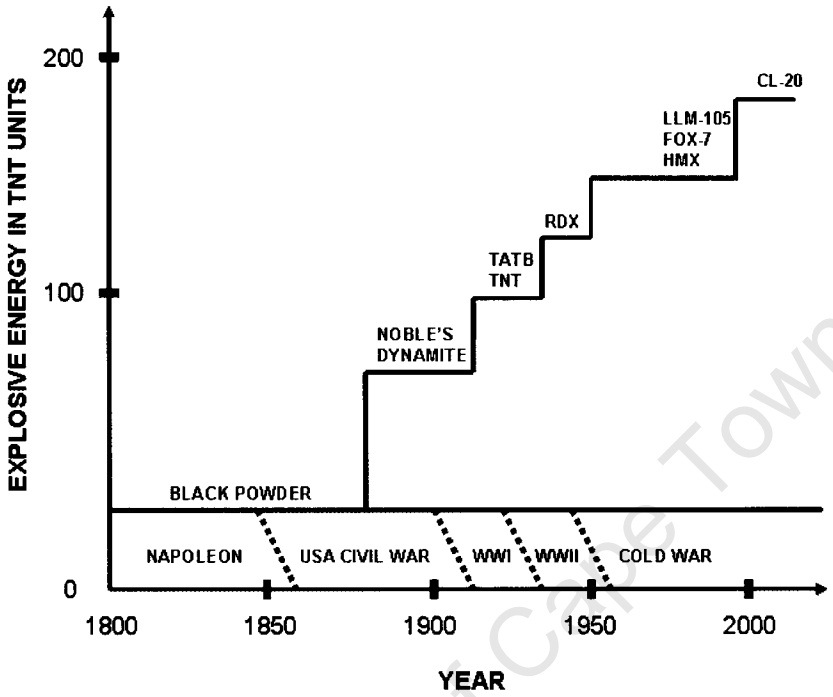

Figure 2.2 The evolution of military explosives (Souers [14])

Table 2.1 provides a relative type of comparison in terms of density, velocity and pressure characteristics of the most recently developed explosives since WWII as illustrated in **Figure 2.2**.

Table 2.1 Explosive characteristics (Souers [14])

TYPE OF EXPLOSIVE	DENSITY OF EXPLOSIVE, ρ (g/cm^3)	VELOCITY OF DETONATION, v (m/s)	PRESSURE OF DETONATION, P_{CJ} (GPa)
TATB	±1.93	±7760	±31.2
FOX-7	±1.88	±8870	±35.9
CL-20	±2.04	±9380	±42.1
LLM-105	±1.92	±8730	±35.9
TNT	**±1.60**	**±6500**	**±28.4**

TNT, or trinitrotoluene, is today still the most used high explosive and thus an important military explosive. TNT was discovered in 1863 as a dye agent. It was not used as an

explosive until 1904. It became popular as a military explosive during World War I and it became the standard military explosive by World War II. The power of other explosives is frequently expressed as an equivalent amount of TNT. It can be cast easily by melting the material and then pouring it into shells or mine casings. It is very stable and can be stored for long periods. It is extremely moisture resistant and is not likely to be detonated by physical shock.

2.4 The Southern African TM-57 blast mine threat

The most common used anti-vehicular mines are the so called "blast mines" which contain a large amount of explosive material and produce the damage/destruction of the target by ***blast loading***.

2.4.1 Definition of a mine

To understand the operation of a mine requires quoting a proper definition of a mine as well as how such a destructive weapon (munitions) is deployed. Fields [15] defines an anti-vehicular mine as ***a device that is placed onto or into the ground and explodes when triggered by a vehicle***.

Figure 2.3 illustrates the configuration of a Chinese Type 72 S1 mine. The following are components of a typical mine:

- **Body**: A component manufactured from either metal, plastic or wood, which encases and protects the mine with its attachments;
- **Ignitor**: A device which responds to an initiating action, such as pressure, to start the explosive train by activating the detonator;
- **Detonator**: A detonator is a sensitive device containing a detonating charge that is used for initiating detonation in the booster charge. A blasting cap (Electric or Non-Electric) is often used to denote a detonator;
- **Booster charge**: A less sensitive high explosive (detonate by fast supersonic reaction) which amplifies the small detonation from the detonator to the level which will detonate the main charge, and

- **Main charge**: A high explosive charge, which upon detonation, accomplishes the purpose of the mine by attacking the target with blast and fragments. TNT is a common explosive found in landmines throughout the world.

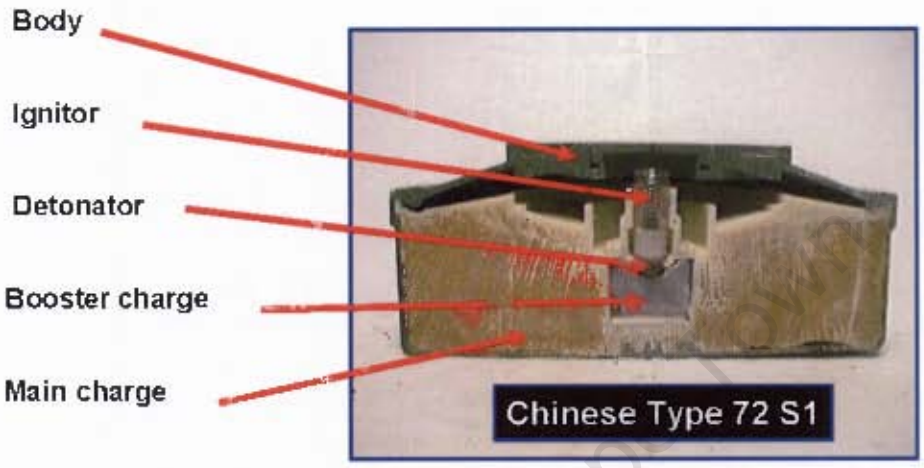

Figure 2.3 Components of a typical mine (Source unknown)

2.4.2 Classification of mines

Mines are containers of explosive material and are classified in South Africa as either anti-personnel mines or anti-tank (anti-vehicular) mines as indicated in **Figure 2.4**:

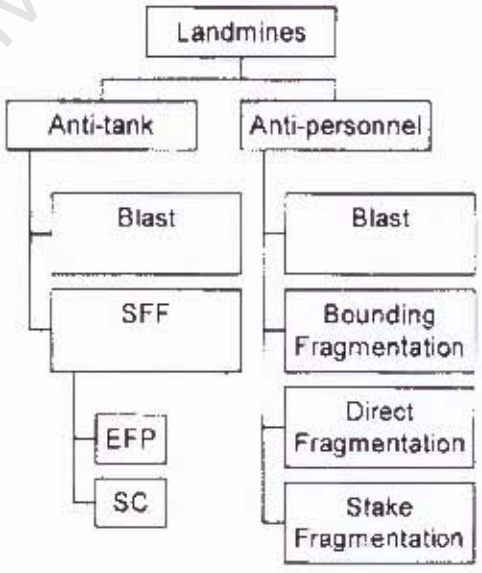

Figure 2.4 South African mine classification (excluding IEDs) (Nell [5])

2.4.3 Deployment of anti-vehicular mines

Mines in general range from a crude wooden box loaded with dynamite to sophisticated "magnet-sensitive" mines that can be calibrated to explode under the weakest part of a vehicle. Mines are designed to be hand-buried, dropped from aircraft, or fired from a cannon-like "mine projector," which can hurl mines up to 36 metres (Dewing and Koerner [16]). A landmine can be triggered using different techniques such as ***pressure, movement, sound, magnetism*** **and** ***vibration***. The new generation of sophisticated mines is able to sense the difference between friend and foe types of vehicles by way of a built-in signature capability. This will theoretically enable friendly forces to use the mined area while denying the enemy access to this area. Army engineers combine the main trigger with a touch or tilt trigger, to prevent the enemy from defusing it. Many landmine designs are now using as little metal as possible to make searching with metal detectors more difficult. Fields [15] states that new generation mines are designed to self-destruct after a period of weeks or months to reduce the likelihood of civilian casualties at the conflict's end. ***According to this source, these self-destruct mechanisms are not reliable and it is a known fact that most landmines laid historically in the African continent are not equipped in this manner***.

Figure 2.5 indicates the various schemes of mine deployment, else called methods of emplacement. Position (a) indicates a position on top of the soil, whilst position (b) indicates a position flush with the soil surface and position (c) indicates a mine shallow-buried in soil. Depths of burial generally vary between 50 mm – 200 mm. ***Of special interest for this dissertation is the blast loading considering the mine flush with the soil surface (position b) or below the soil surface (position c)***.

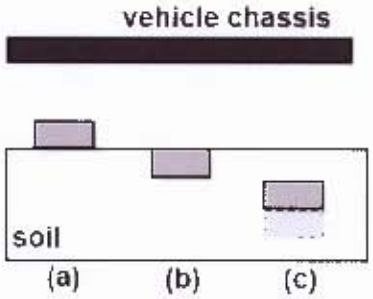

Figure 2.5 Scheme of landmine deployment (Fišerová [17])

2.4.4 Characteristics and functioning of the TM-57 anti-vehicular mine

The TM-57 is a large, metal-cased anti-tank (AT) blast mine as illustrated in **Figure 2.6**. It was developed from the TM-46 to incorporate a larger charge and improved fusing. The cylindrical body has a stepped pressure plate with a central threaded fuse well, sealed with a threaded plug during transit. The lower section of the body contains the main charge around a large central booster, with an air gap between the encased explosive and the pressure plate. On the side of the mine is an auxiliary fuse well with a booster, threaded to accept "MUV" or "VPF" type fuses to give the mine an anti-lift capability. The base of the mine has seven stamped reinforcing ribs, a steel carrying handle and one or two filling plugs.

Table 2.2 summarises the characteristics of the TM-46, TM-57 and TM-62 anti-vehicular mines. The evolution of the range of mines started with the TM-46 and ended with the TM-62.

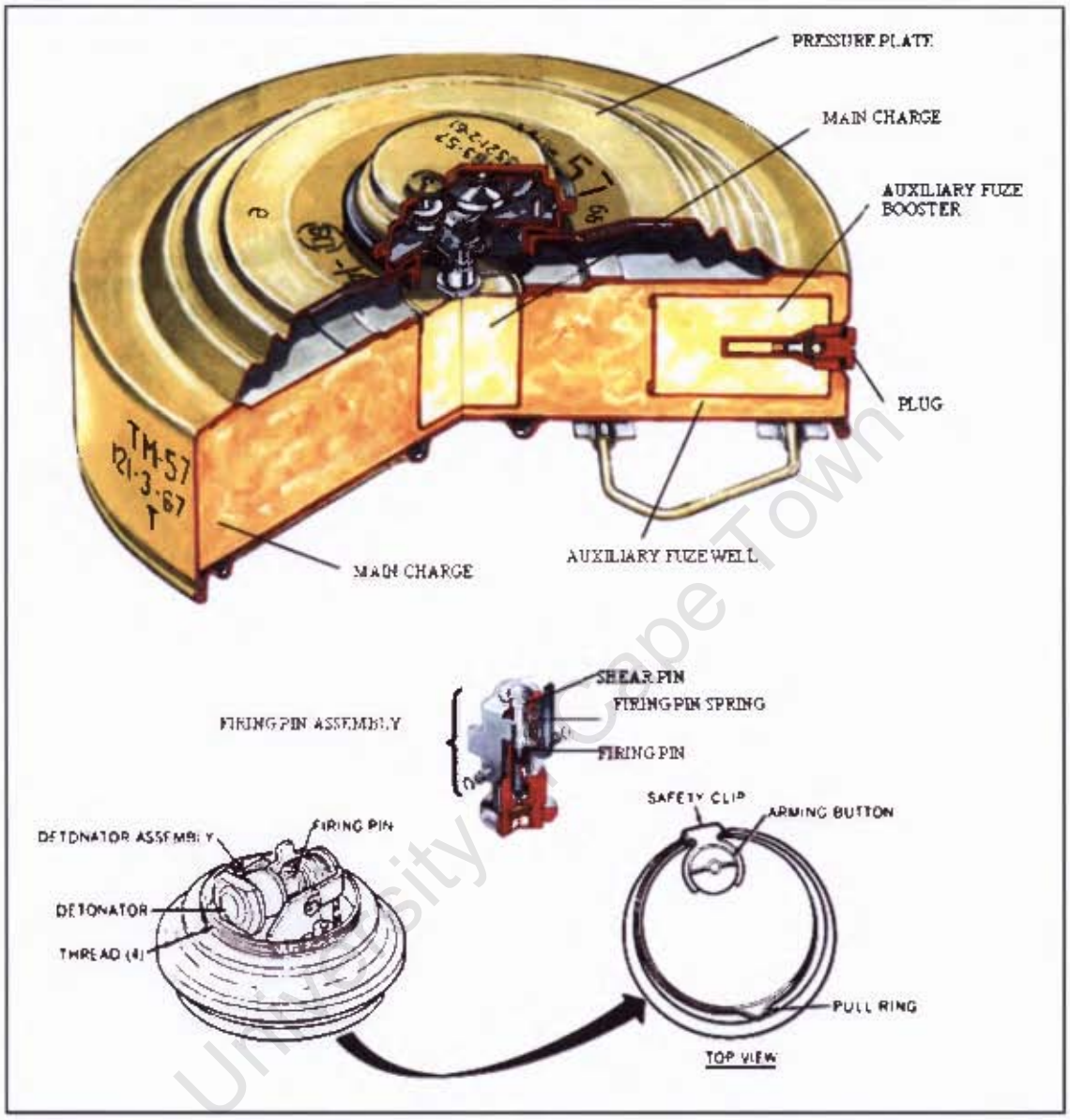

Figure 2.6 Cutaway diagram of the TM-57 mine with details of the fuse mechanism (Canadian Forces Landmine Database [18])

Table 2.2 Characteristics of the TM-46, TM-57 and TM-62 family of mines (Canadian Forces Landmine Database [18])

	TM-46	TM-57	TM-62M
1	Weight:8,6 kg	Weight:8,47 kg	Weight:9,5 kg
2	Explosive weight:5,7 kg	Explosive weight:6,9 kg	Explosive weight:7,5 kg
3	Height:94 mm	Height:119 mm	Height:128 mm
4	Diameter:305 mm	Diameter:312 mm	Diameter:320 mm
5	Explosive type:TNT	Explosive type:TNT	Explosive type:TNT
6	Fuses: Pressure: MV-5, MVM Tilt-rod: MVSh-46	Fuses: Pressure: MVZ-57 Tilt-rod: MVSh-47	Fuses: MVZ-62, MVCh-62, MVN-62, MVN-72, VM-62Z, MWP-62 (for TM-62P)
7	Operating pressure: 120 to 400 kg (21 kg tilt)	Operating pressure: 120 to 400 kg (21 kg tilt)	Operating pressure: 150 to 550 kg
8	Colour:Olive green	Colour:Olive green	Colour:Olive green
			
	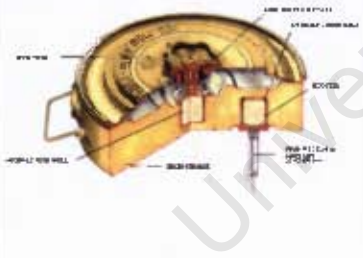	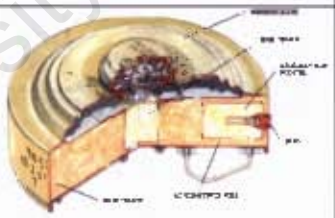	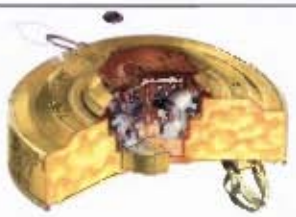

Figure 2.7 illustrates the typical scene directly after an anti-tank vehicle mine incident. Note the excessive damage to the overturned vehicle and number of vehicle parts around the scene.

Figure 2.7 Vehicle casualties due to a mine blast (Sponfeldner [19])

The difference between theory and
practice is a lot bigger in practice
than in theory.
— Peter van der Linden

3 LITERATURE REVIEW FOCUSSING ON BLAST LOADING PHENOMENA OF ANTI-VEHICULAR MINES (PRIMARY FOCUS) AND IMPROVISED EXPLOSIVE DEVICES AS A THREAT TO MINE-PROTECTED VEHICLES

3.1 Introduction

The first objective requires the scanning of open literature for information on anti-vehicular mine explosions close to, on the ground or shallow-buried in soil.

In executing this objective this chapter will review and conclude on the literature found to gain an understanding of the blast loading phenomena of anti-vehicular mines and improvised explosive devices as a threat to mine-protected vehicles.

The ***first part of this chapter will concentrate on certain basics and principles***, namely:

- Defining a chemical explosion;
- Ideal blast (shock) wave behaviour;
- Formation of a blast (shock) wave in an ideal gas using shock tube experiments to explain the basics;
- Ideal blast pressure-time history to explain the idealistic behaviour of air pressure expansion and cooling over a very short time;
- Blast-wave scaling;
- Blast-wave diffractions and reflections in terms of normal, oblique and mach stem formations, and
- Explosive material expressed in terms of TNT equivalent mass.

The ***second part of this chapter will elaborate on close to or on the ground (reflective plane) detonated high-explosives (unconfined explosions)*** and explain the phenomena as per:

- Kinney and Graham empirical equations; Reflected peak pressure and reflection coefficient illustrated by an example for a 10.19 kg TNT explosive charge detonated on a reflective plane measured at a standoff distance of 500 mm above ground level;
- Reflected pressure effected by the angle of incidence; blast curves for hemispherical ground burst TNT high-explosive spherical charges illustrated with an example for a 10.19 kg TNT explosive charge detonated on a reflective plane measured at a standoff distance of 500 mm above ground level;
- Compare all the 10.19 kg TNT explosive-charges example results with the CONWEP™ and AUTODYN™ results obtained from Fišerová et al [12], and
- Describe the effect of an IED and demonstrate the principles with an example.

The ***third and last part of this chapter will investigate shallow-buried high-explosive charges detonated in soil (confined explosions)*** to more accurately explain mine-protected vehicle mine explosions in terms of:

- The distinctive differences (phenomena) between high-explosive charges detonated on a reflective plane and detonated shallow-buried in soil;
- The interaction of soil, detonation products and air in producing the blast loads for near-field (close-in) targets;
- Detail discussions of all the known parameters influencing the blast load on a near-field (close-in) target;
- Explanation of the loading mechanisms, and
- The illustration of all the effects combined on a mine-protected-vehicle by means of an integrated vehicle blast-loading model.

(Appendix A contains all the important definitions, such as stagnation pressure, static overpressure, dynamic pressure, etc.)

3.2 Defining a chemical explosion

Smith and Hetherington [20] define a chemical explosion as ***a rapid oxidation of fuel elements (carbon and hydrogen atoms)*** contained within the explosive compound. They claimed the oxygen needed for this reaction is contained within the compound, which implies that the presence of air is thus not necessary. To be useful, a chemical explosive must only explode when it is required to do so and should, under normal conditions, be inert and stable. The ***rate of reaction*** according to Smith and Hetherington [20] will determine the usefulness of the explosive material for practical applications. Most practical explosives are ***'condensed'***, meaning they are either ***solids or liquids***.

Despite the claims of Smith et al that all the oxygen required is contained in the explosive compound, a ***chemical reaction is rarely stoichiometric***, and ***in most cases there is insufficient oxygen to complete the reaction***. In practice this is very noticeable when TNT explodes and releases excessive black smoke indicating unburned carbon which is then followed by a yellow flame. This yellow flame is afterburn and continued chemical reaction when the detonation products expand and ingest new oxygen (Bergeron [21]). Interestingly this phenomenon is supported by Renfroe [22] who found that only ***about one-third of the total chemical energy available in most high-explosives is released in the detonation process. The remaining two-thirds are released more slowly as the detonation products mix with air and burn. She states that the after-burning process has little effect on the initial blast-wave properties because it is much slower than detonation.***

3.3 Defining a blast (shock) wave

When detonation occurs in the explosive material, the shock so formed is called a ***detonation wave***. When an explosion occurs in air, the shock wave so formed is termed a ***blast-wave*** and comprises of highly compressed air (Smith and Hetherington

[20]). Physically the front of a wave as illustrated in **Figure 3.1**, called the blast or shock front, ***is like a wall of highly compressed air and has an overpressure much greater than that in the region behind it***. This peak overpressure decreases rapidly however as the blast or shock wave is propagated outward. ***A blast-wave front possesses characteristics similar to a one-dimensional shock wave created by a shock tube***.

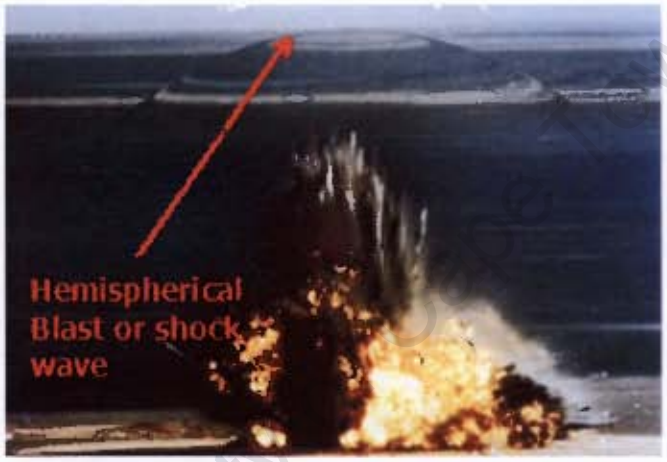

Figure 3.1 A large chemical explosion with a perfectly uniform blast-wave front (DSTO Australia [23])

3.3.1 The physics of the formation of a blast (shock) wave in an ideal gas, ignoring any wave reflections

When the gas molecules accelerate towards supersonic speed (i.e. greater than the sound speed which is estimated at approximately 344 m/s at 21°C and at sea level for air), the pressure, density and temperature build up (steep gradients) ahead of this disturbance. This situation is analogous to the case of a ship moving through water at a speed greater than the velocity of the surface waves on the water. The water tends to pile up ahead and to both sides of the bow, forming a steep wave of large amplitude known as a bow-wave. This water wave is stationary relative to the ship, diverges linearly, and becomes attenuated with increasing distance backwards from the bow. ***Such a wave, when generated in air by a supersonic disturbance such as an***

explosion, is termed a blast-wave front and has very very steep gradients of pressure (The Centre for Explosion Studies [24]).

3.3.1.1 Normal 1-D blast (shock) wave front equations

A blast-wave impact on a target comprises dynamic loading. A target subjected to dynamic loading cannot be tested easily since such tests are expensive and difficult to repeat. ***While "shock waves" are different from "blast-waves" in possessing a different profile, i.e. pressures behind the wave as well as pressure drop in the case of a blast-wave is unlike a shock wave in which the pressure remains constant, a shock wave impacts still provide a reasonable simulation of the blast-wave during an explosion. This is because the damage is caused by the impacting pressure or so called wave front (Rousseau et al [25])***.

With the principles of a shock (blast-wave front) being introduced, the physical nature of a shock tube and its application will now be discussed. Equations will be derived for a 1-D shock wave by means of a shock tube model in a gaseous medium. ***A shock tube is a device used primarily to study shock effects on structural materials. Understanding the science behind shock waves can improve blast-wave attenuation research***.

The shock tube that will be described consists of an enclosed cylinder divided into two sections by a gas tight diaphragm, specifically to obtain similar reflections as will be experienced by a mine-protected vehicle (**Figure 3.2** refers). The shock tube consists of two main sections, the driver (high-pressure side) and driven (low pressure side) sections. A pressure difference is applied to the diaphragm causing it to rupture, creating a contact surface (slip surface) between the high and low pressures. A normal one-dimensional shock wave arises from the pressure discontinuity and propagates into the driven section at Mach number **M**. At the initial instant when the diaphragm is burst, the pressure distribution is ideally a step function. Across this contact surface velocity and pressure are equal but perhaps not the temperature and density. As the shock wave

(***known as the incident shock wave***) progresses along the shock tube, it raises pressure and temperature to higher values. Simultaneously, a rarefaction or Taylor wave, often referred to as an expansion fan, travels back into the driver gas and the reflection is then called the reflected expansion fan. When the shock wave arrives at the boundary surface, it reflects, further increasing pressure and temperature.

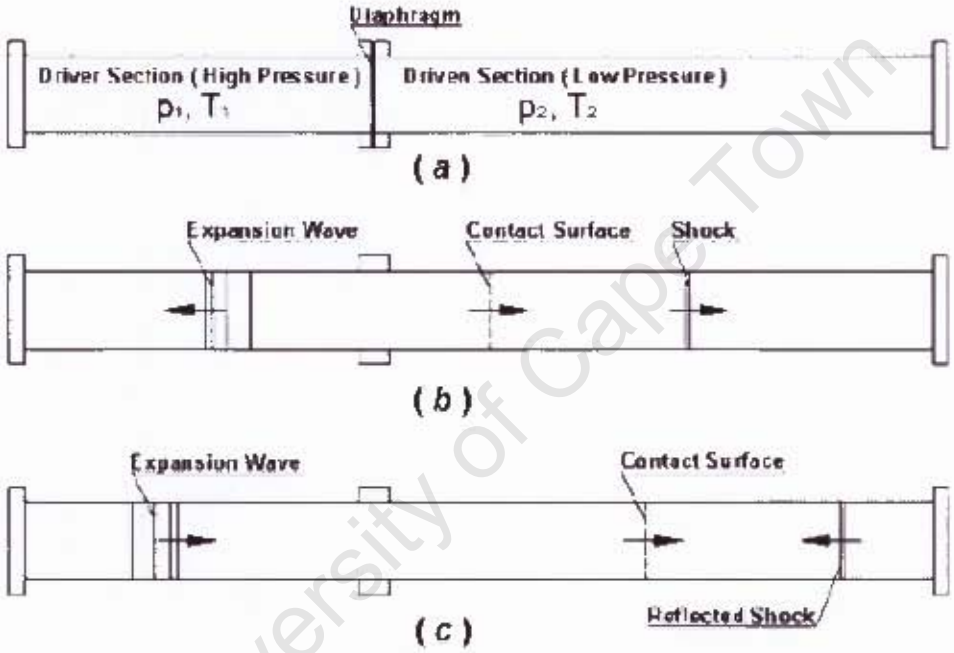

Figure 3.2 Simple shock tube with both ends closed. Figures (a), (b) and (c) indicate the different stages of shock wave progress and reflection when it strikes the end. (Rousseau et al [25])

The motion of the gas and the waves within the shock tube are represented by a displacement – time (x – t) diagram as indicated in **Figure 3.3**. The wave pattern consists of a shock wave propagating into the driven gas which is at first at rest. According to Rousseau et al [25]) ***the state of the gas after passage of the shock wave is one of uniform pressure and uniform gas velocity***.

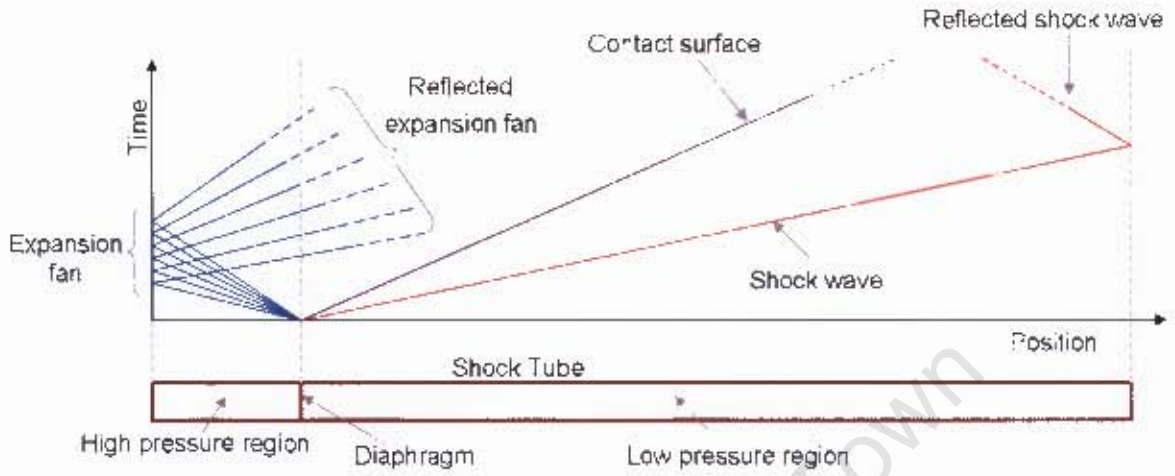

Figure 3.3 Motion in a shock tube represented by a position-time diagram (Wikipedia [26])

The following assumptions are made in the basic theory of shock waves (The Centre for Explosion Studies [24]):

- The gas flow is one-dimensional;
- The gas is ideal and has constant specific heats;
- Heat transfer and viscosity effects are neglected, and
- Diaphragm rupture of the shock tube system is instantaneous and does not disturb the subsequent gas flow.

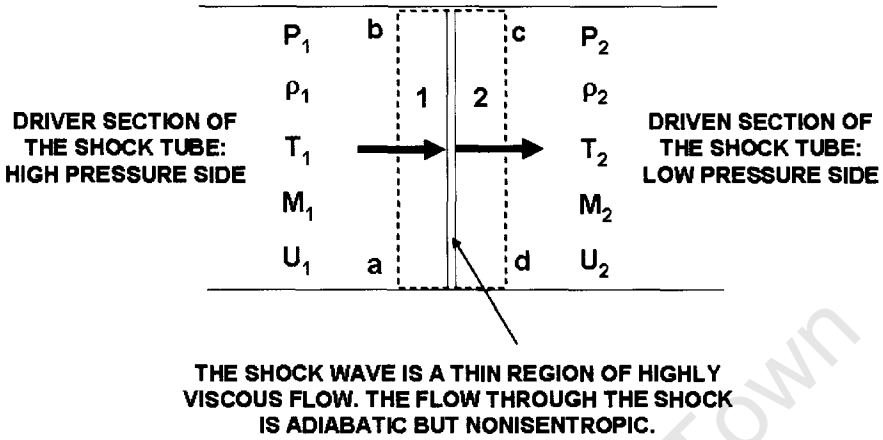

Figure 3.4 Sketch of a shock wave and shock frame. Velocities indicated upstream and downstream of the shock wave are with respect to shock wave (Rousseau [25])

The states upstream (by convention *state 1* - driver section: high-pressure side of the shock tube) and downstream (by convention *state 2* - driven section: low-pressure side of the shock tube) of a shock wave are ***related by the conservation laws of elementary physics***. The relationships are referred to as the "***jump conditions***" because they specify the apparent jumps in properties that occur across shock waves when they are ***considered as discontinuities***. These jumps are a function of the strength of the waves, usually measured in terms of wave speed, the state 1 upstream of the wave (driver section: high-pressure side of the shock tube), and the equation of state for the substance (Shepherd [27]). The jump conditions will be derived by considering propagating shock waves. Using the basic conservation equations, the one-dimensional equations for a constant area equilibrium flow with two regions (1 and 2) separated by a non-equilibrium region as per **Figure 3.4** are:

Conservation of mass:

$$\rho_1 \cdot U_1 = \rho_2 \cdot U_2 \qquad (3.1)$$

Conservation of momentum:

$$P_1 + \rho_1 \cdot U_1^2 = P_2 + \rho_2 \cdot U_2^2 \tag{3.2}$$

Conservation of energy:

$$H_1 + \frac{1}{2} \cdot U_1^2 = H_2 + \frac{1}{2} \cdot U_2^2 \tag{3.3}$$

The specific enthalpy **H** is defined as:

$$H = E + R \cdot T \tag{3.4}$$

The entropy of the shocked fluid (state 2) will be greater than or equal to that of the initial fluid (state 1) (Shepherd [27]).

Using the basic assumption that the gas is ideal and has constant specific heats gives:

$$\gamma = \frac{C_p}{C_v} \tag{3.5}$$

The following thermodynamic relations also hold for an ideal gas:

$$H = C_p \cdot T \tag{3.6}$$

$$R = C_p - C_v \tag{3.7}$$

From (3.5), (3.6) and (3.7):

$$H = \frac{\gamma \cdot R \cdot T}{\gamma - 1} \tag{3.8}$$

or, by using the equation of state of ideal gases (ideal gas law), PV = RT or P = ρRT, this becomes:

$$H = \frac{\gamma \cdot P}{(\gamma - 1) \cdot \rho} \tag{3.9}$$

By applying the equations (3.1) to (3.9), the following relations are derived for the changes in pressure, density and temperature across the shock:

The pressure ratio across the shock wave may be written as:

$$\frac{P_2}{P_1} = \frac{2 \cdot \gamma \cdot M_1^2 - (\gamma - 1)}{(\gamma + 1)} \tag{3.10}$$

The density ratio between the two sides of the shock is:

$$\frac{\rho_2}{\rho_1} = \frac{(\gamma + 1) \cdot M_1^2}{(\gamma - 1) \cdot M_1^2 + 2} \tag{3.11}$$

The temperature ratio between the two sides of the shock is:

$$\frac{T_2}{T_1} = \frac{\left[2 \cdot \gamma \cdot M_1^2 - (\gamma - 1)\right]\left[(\gamma - 1) \cdot M_1^2 + 2\right]}{(\gamma + 1)^2 \cdot M_1^2} \tag{3.12}$$

The shock Mach number of the fluid upstream is defined as:

$$M_1 = \frac{U_1}{a_1} \tag{3.13}$$

The speed of sound in the upstream region:

$$a_1 = \sqrt{\gamma \cdot R \cdot T_1} \tag{3.14}$$

If the initial conditions, *state 1*, of pressure **P**, density ρ and temperature **T** are known together with the shock velocity **U**, then the elevated conditions behind the shock, *state 2*, can be calculated from the above relations in an ideal gas ***to represent a typical blast-wave during an explosion***.

3.3.1.2 Summary of the characteristics of a blast (shock) wave ([28])

- They all create very large changes in local pressure over very short times;
- They self-steepen into blast-wave fronts;
- They are non-linear waves that abruptly change the state of the supersonically approaching gas by increasing its temperature, and
- The narrow region called the blast-wave front is a region where thermodynamically processes are irreversible.

3.3.2 Idealised blast pressure-time history

A fixed point in air outside the scaled radius of ±0.8 m/kg$^{1/3}$ of the detonation products (Fišerová et al [12]), exposed to the passage of a blast-wave, will experience a pressure variation with time that rises sharply to a maximum value, corresponding to the arrival of the blast-wave front, and then diminishes slowly with time as the blast-wave front continues on and the pressure drops off towards regions with lower pressure, i.e. atmospheric pressure. There will also be a point where the pressure drops below ambient and this is referred to as the negative or suction phase of the air blast. Finally, equilibrium will be reached with atmospheric pressure. ***The precise shape of the pressure-time curve is dependent on the mode of production of the blast-wave and on the distance from the source of the disturbance (explosion) to the point of observation***. For mine blast effects, it is the positive phase pressure history that is of greatest concern and interest (Braid [1]).

An ideal pressure-time history graph for an explosive-charge blast-wave is shown in **Figure 3.5**. At arrival time $\mathbf{t_A}$, following the explosion, pressure at that position suddenly increases to a peak value of incident or static overpressure, $\mathbf{P_{SO}}$, over the ambient pressure $\mathbf{P_a}$. The pressure then decays to ambient level at time $\mathbf{t_G}$, then decays further to an under pressure (creating a vacuum) before eventually returning to ambient conditions at $\mathbf{t_N}$. The quantity $\mathbf{P_{SO}}$ is referred to in various ways such as ***peak incident***

overpressure, peak static overpressure or merely peak overpressure (Smith and Hetherington [20], Heffernan [29], Kinney and Graham [30] and Ngo et al [31]).

In addition to blast pressure, the other important parameter more related to damage is the positive phase impulse, i_{so}, ***which is simply the integral of pressure during the positive phase,*** that is duration t_o (Smith and Hetherington [20]).

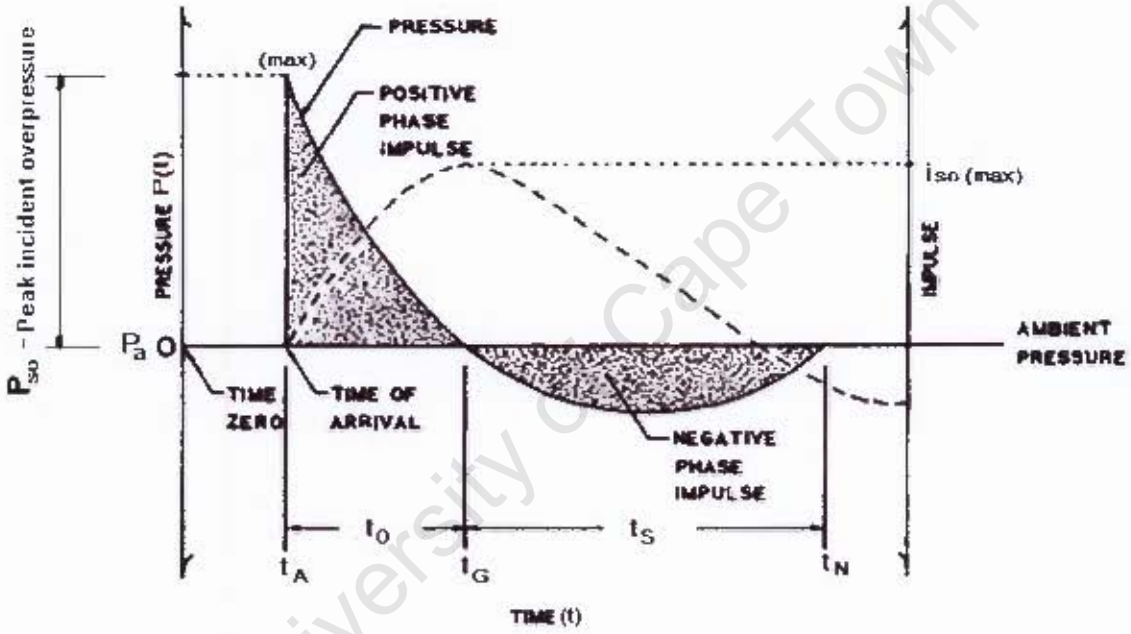

Figure 3.5 Ideal blast-wave depicting pressure and impulse – time history (Braid [1])

3.4 High-explosive charges detonated in free air

Many mathematical forms have been suggested to capture the time variation of these blast-waves in free air (Stuhmillar [32]). The pressure-time history is described by an ***exponential function such as the Friedlander wave equation which represents a theoretical free-air explosion wave of the positive phase*** (i.e. $t<t_o$) of a spherical chemical charge at the ***medium to far field*** (Heffernan [29]):

$$P(t) = P_{so}\left[1 - \frac{t}{t_o}\right]e^{\left(\frac{bt}{t_o}\right)} \qquad (3.15)$$

The high peak overpressure will over time decrease rapidly as the blast-wave front is propagated outward with increasing distance typically with decay constant "**b**". By selecting a value for the dimensionless constant **b**, various pressure–time histories can be described. Lam et al [33] propose the graph as illustrated in **Figure 3.6** to select the value of the dimensionless (positive) constant "**b**" with scaled distance **Z** (paragraph 3.4.1 Blast-wave scaling refers), called the "waveform parameter". ***Kinney and Graham [30] states that the "wave form parameter" b may also be regarded as an "adjustable factor" which is selected so that the overpressure-time relations provide more suitable values of blast pressure.***

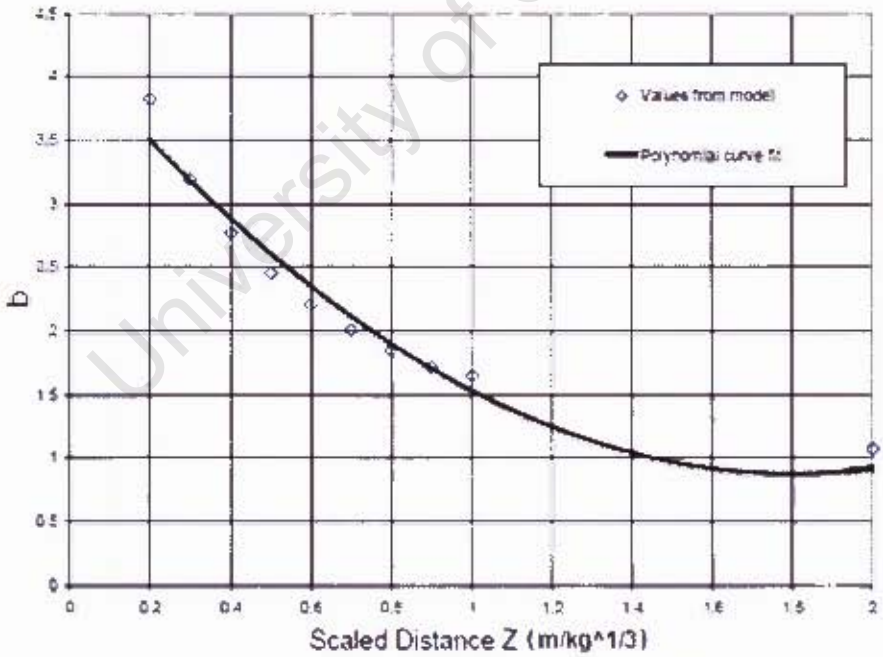

Figure 3.6 Correlation of wave form parameter "b" with scaled distance Z (Lam et al [33])

According to Lam et al [33] the explicit correlation between "b" and "Z" as shown in Figure 3.6 facilitates the computation of the pressure function for

any given blast scenario that fits the given scaled distances, Z, of 0.2 and 2 m/kg$^{1/3}$. This is suitable for cases such as an anti-vehicular mine explosion of 8 kg TNT at a standoff distance of 0.5 m (Z = 0.25 m/kg$^{1/3}$) as well as for an IED explosion of 50 kg at a standoff distance of 5 m from a mine-protected vehicle (Z = 1.36 m/kg$^{1/3}$).

According to the authors the quadratic curve-fit is a reliable fit and is given by the following equation:

$$b = Z^2 - 3.7 \cdot Z + 4.2 \tag{3.16}$$

The area under the pressure-time graph of **Figure 3.5** is called the "Impulse of the Wave" and is an important parameter related to damage, also called the positive phase specific impulse:

$$i_{SO} = \int_{t_A}^{t_A + t_O} P(t)\,dt \tag{3.17}$$

3.4.1 Blast-wave scaling (often called cube-root scaling)

Hopkinson (1915) and Cranz (1926) independently published the most common form of blast-wave scaling (Smith and Hetherington [20]). Sachs scaling can be used to relate blast-wave properties in two different sets of atmospheric conditions, or to convert experimental data to equivalent blast-wave properties at standard atmospheric conditions (Smith and Hetherington [20]). Hopkinson – Cranz or cube-root is the simplest and most common form of scaling, but is only applicable to identical explosive types and charge shapes. Baker [34] states that Dewey and Sperazza studied the detonation of bare pentolite spheres in an altitude simulation chamber so as to vary temperature and pressure. The Hopkinson – Cranz scaling law was shown by Dewey and Sperazza to be consistent for distance changes, but not for altitude changes, i.e. ambient pressure changes, while Sachs's scaling law produced excellent scaled results that were consistent for changes in both distance and altitude.

According to Smith and Hetherington [20] Hopkinson – Cranz scaling law is a special case of Sachs's scaling law. This is explained by Baker [34] in that Sachs's scaling law reduces to the Hopkinson – Cranz scaling law when there is ***no atmospheric pressure change*** between the explosive test data and the actual condition of the desired explosive for which one is predicting the air blast parameters.

Olatidoye et al [35] state that self-similar blast-waves are created at equal scaled distances when two of the same type of explosive charges of different masses but similar geometry are detonated in the identical atmospheric conditions.

Smith and Hetherington [20] state that a scaled range parameter, **Z**, is used to relate the distance from the two explosive charges, namely:

$$Z = \frac{R}{\sqrt[3]{E}} \tag{3.18}$$

But:

$$E \propto W$$

Therefore:

$$Z = \frac{R}{\sqrt[3]{W}} \tag{3.19}$$

Figure 3.7 illustrates graphically the concept of cube-root scaling. The same scaled distance of $15 m/kg^{1/3}$ can be achieve for 100 kg TNT placed at a standoff distance of 68 m versus 10 kg TNT placed at a standoff distance of 32 m. **Z** is then the constant of proportionality in this illustration.

Reflection phenomena can be divided into two categories, namely normal reflections and oblique reflections:

3.4.2.1 Normal reflections

Normal reflections occur when the blast-wave hits the object head on, or ***at zero degrees*** incidence.

3.4.2.2 Oblique reflections

Oblique reflections are further subdivided into regular reflections and Mach stem formation as follows:

3.4.2.2.1 Regular reflections

Regular reflections occur when the angle of incidence is small, ***<40 degrees*** in air (Smith and Hetherington [20]). The angle of reflection is not normally the same as the angle of incidence for oblique reflections (Kinney [37]) and the discrepancy depends on the pressure of the wave.

3.4.2.2.2 Mach stem formation

Mach stem formation occurs for larger angles of incidence (***>40 degrees***). A "spurt type effect" occurs when the shock front impinges on the surface at near grazing incidence (Kinney [37]). The grazing incidence refers to the 40° angle of incidence. The phenomenon occurs as indicated in **Figure 3.8** when the reflecting wave catches up with and fuses with the incident wave to form a third wave front called Mach stem. The place where the three come together is called the triple point (Smith and Hetherington [20]).